



HAL
open science

'Flash' Synthesis of CdSe/CdS Core-Shell Quantum Dots

Marco Cirillo, Tangi Aubert, Raquel Gomes, Rik van Deun, Philippe Emplit, Amelie Biermann, Holger Lange, Christian Thomsen, Edouard Brainis, Zeger Hens

► **To cite this version:**

Marco Cirillo, Tangi Aubert, Raquel Gomes, Rik van Deun, Philippe Emplit, et al.. 'Flash' Synthesis of CdSe/CdS Core-Shell Quantum Dots. *Chemistry of Materials*, 2014, 26 (2), pp.1154-1160. 10.1021/cm403518a . hal-03760499

HAL Id: hal-03760499

<https://hal.science/hal-03760499v1>

Submitted on 25 Aug 2022

HAL is a multi-disciplinary open access archive for the deposit and dissemination of scientific research documents, whether they are published or not. The documents may come from teaching and research institutions in France or abroad, or from public or private research centers.

L'archive ouverte pluridisciplinaire **HAL**, est destinée au dépôt et à la diffusion de documents scientifiques de niveau recherche, publiés ou non, émanant des établissements d'enseignement et de recherche français ou étrangers, des laboratoires publics ou privés.

'Flash' Synthesis of CdSe/CdS Core-Shell Quantum Dots

Marco Cirillo,^{†,‡} Tangi Aubert,^{†,‡} Raquel Gomes,^{†,‡} Rik Van Deun,[§] Philippe Emplit,^{||} Amelie Biermann,[‡] Holger Lange,[‡] Christian Thomsen,[‡] Edouard Brainis,^{†,‡} Zeger Hens^{†,‡,*}

[†] Physics and Chemistry of Nanostructures, Ghent University, Krijgslaan 281-S3, 9000 Ghent, Belgium.

[‡] Center for Nano- and Biophotonics (NB-Photonics), Ghent University, Belgium.

[§] L³ – Luminescent Lanthanide Lab, f-element coordination chemistry, Ghent University, Krijgslaan 281-S3, 9000 Ghent, Belgium.

^{||} OPERA Department, Université Libre de Bruxelles, Brussels 1050, Belgium.

[‡] Institut für Festkörperphysik, Technische Universität Berlin, Hardenbergstr. 36, 10623 Berlin, Germany

KEYWORDS: *semiconductor, nanocrystals, giant core/shell, Raman, non-blinking*

ABSTRACT: We report on the 'flash' synthesis of CdSe/CdS core-shell quantum dots (QDs). This new method, based on a seeded growth approach and using an excess of a carboxylic acid, leads to an isotropic and epitaxial growth of a CdS shell on a wurtzite CdSe core. The method is particularly fast and efficient, allowing the controllable growth of very thick CdS shells (up to 6.7 nm in the present study) in no more than 3 minutes, which is considerably shorter than in previously reported methods. The prepared materials present state-of-the-art properties with narrow emission and high photoluminescence quantum yields, even for thick CdS shells. Additionally, Raman analyses point to an alloyed interface between the core and the shell, which, in conjunction with the thickness of the CdS shell, results in the observed considerable reduction of the blinking rate.

Quantum dots (QDs) show unique optical properties that make them a widely studied material for applications in several fields such as photonics, optoelectronics and biotechnology.¹⁻⁴ However, due to their nanometer size, the optical properties of QDs are strongly dependent on the properties of their surface. For instance, surface defects and poor surface passivation with organic ligands can lead to enhanced trap state emission or non-radiative recombination and consequently to a low photoluminescence quantum yield (PLQY) and photobleaching.⁵ Moreover, an undesired characteristic of many semiconductor QDs is the on-off blinking of their emission. This blinking behavior has been extensively studied and is often explained by the recombination of electron-hole pairs through Auger processes.^{6, 7} To overcome these issues, the design of heterostructures such as core-shell QDs has been widely investigated. Indeed, capping QDs with a larger bandgap material results in an improved surface passivation and a better confinement of the excited carriers, thus decreasing trap emission and increasing PLQY. Core-shell structures have also proven to be very promising for non-blinking QDs.⁸⁻¹³ In particular, for CdSe/CdS core-shell QDs both the presence of large CdS shells¹⁰⁻¹² and alloyed interfacial layers¹³ have been reported as efficient ways to decrease Auger recombination, and consequently reduce or even suppress blinking.

Several procedures have been developed for the synthesis of CdSe/CdS core-shell QDs, including continuous or layer-by-layer shell growth.^{11, 14, 15} The most widely spread method is probably the successive ion layer adsorption and reaction

process (SILAR), a layer-by-layer approach that allows for a precise tuning of the shell thickness and that has been successfully used for the synthesis of so-called 'giant' CdSe/CdS QDs featuring more than 10 CdS layers.^{10, 12, 16} Many efforts have been devoted in the past years toward a better understanding of the synthetic parameters of this SILAR procedure in order to achieve optimal morphological and optical properties.^{12, 16, 17} However, this method remains time consuming and complex as different temperatures, annealing times, or precursor concentrations are required depending on the deposited element (Cd or S), the core size, or the number of CdS layers.^{12, 16, 17} Although 'giant' CdSe/CdS QDs were successfully synthesized with annealing times of 20-30 minutes per CdS layers,¹⁶ Ghosh *et al.* recently reported that optimal optical properties could only be achieved with annealing times of 3.5-4 hours per CdS layers,¹² which corresponds to more than two days of continuous synthesis to grow 15 CdS layers. In addition, this method uses relatively low temperatures (below 250 °C). This can lead to residual strain and defects, two elements known to deteriorate PLQY¹⁸⁻²⁰ and promote blinking of the QDs.²¹

Here we report a new, fast and efficient method for the synthesis of CdSe/CdS dot-in-dot QDs. This method, denoted as 'flash' synthesis, consists of a seeded growth at relatively high temperature (330 °C). This approach is adapted from a procedure reported in the literature for the synthesis of anisotropic heterostructures such as CdSe/CdS dot-in-rods²² and tetrapods,^{23, 24} but which was also extended to the synthesis of (ZnSe/CdS)/CdS heterostructured nanorods.²⁵ In the present work, the method was modified to promote the isotropic

growth of CdS shells on CdSe seeds through the use of a carboxylic acid instead of phosphonic acids. With this method, CdS shells with controlled thicknesses of up to 6.7 nm were grown in only 3 minutes while keeping state-of-the-art optical properties. The structure and morphology of the synthesized QDs were characterized by X-ray diffraction (XRD) and transmission electron microscopy (TEM). Raman spectroscopy was used to address the possible alloy formation at the core-shell interface. Finally, the optical properties of the CdSe/CdS QDs were characterized by means of UV-Vis absorption, steady-state and time resolved photoluminescence spectroscopies, highlighting the high PLQY and the low blinking rates of these QDs.

EXPERIMENTAL SECTION

Synthesis of the wurtzite CdSe QDs. CdSe QDs with a wurtzite crystal structure were synthesized according to a procedure described in the literature.²² Briefly, 0.06 g of cadmium oxide (CdO, 99.998% Puratronic, Alfa Aesar), 3 g of tri-octylphosphine oxide (TOPO, 98%, Alfa-Aesar) and 0.280 g of octadecylphosphonic acid (ODPA, 98%, PCI) were mixed in a 25 mL three neck flask. The mixture was heated to 150°C under a vacuum for one hour. The solution was then put under a nitrogen atmosphere and heated to 345°C. As soon as the solution became colorless, indicating the dissolution of CdO, 1.8 mL of tri-octylphosphine (TOP, 97%, Strem) were injected. After the temperature had recovered, a solution containing 0.058 g of selenium (99.999%, Sigma-Aldrich) dissolved in 0.360 g of TOP was injected. The reaction time was varied in order to tune the size of the QDs. Then, the reaction was quenched by a sudden drop of the temperature using a water bath and allowed to cool down to room temperature. The nanocrystals were purified by addition of isopropanol and methanol, centrifugation at 3000 rpm for 10 minutes and re-dispersion in toluene. The purification was repeated three times. The size of the particles was determined from the position of the first excitonic absorption peak using the sizing curve of Mulvaney *et al.*²⁶ The concentration of the QD dispersion was determined based on the absorbance at 350 nm.²⁷

Flash synthesis of the CdSe/CdS dot-in-dot QDs. The synthesis of the CdSe/CdS dot-in-dots was performed by adapting the method developed by Carbone *et al.* for the synthesis of CdSe/CdS dot-in-rods,²² except that a carboxylic acid (oleic acid) was used instead of phosphonic acids. CdO and oleic acid (OA, 90%, Sigma-Aldrich) were mixed with 3 g of TOPO in a three neck flask. The amount of CdO was varied between 0.5 and 3.47 mmol in order to tune the thickness of the CdS shell as detailed in the result section. The OA was introduced with an excess of 4 mmol considering that two equivalents of OA are needed to dissolve one equivalent of CdO. The reaction mixture was heated to 120°C while flushing with nitrogen for one hour. The temperature was then increased to 330°C. As soon as the solution became colorless, 1.8 mL of TOP were injected. After the temperature had recovered, 1.8 mL of a solution containing 87 nmol of CdSe core QDs and sulfur in TOP were injected. The sulfur was always kept in a 3 to 4-fold excess as compared to cadmium. After 3 minutes, the reaction was quenched by a sudden drop of the temperature using a water bath, followed by the injection of 10 mL of toluene. The nanocrystals were purified by the addition of isopropanol and methanol, centrifugation at 3000 rpm for 10 minutes and re-dispersion in toluene. The

purification was repeated three times. The sizes of the core-shell structures were determined by TEM analysis and the numbers of CdS monolayers (MLs) grown were estimated by considering half of the wurtzite CdS *c* lattice parameter (0.3375 nm) as the thickness of one CdS monolayer.

Material characterization. Bright field transmission electron microscopy (TEM) images were taken using a Cs corrected JEOL 2200 FS microscope. The crystal structure of the QDs was determined by X-ray diffraction (XRD), using a Thermo scientific ARL X'TRA diffractometer. XRD samples were prepared by dropcasting a dispersion of QDs in an 80:20 hexane:heptane mixture on a glass slide. Absorption spectra were taken using a Perking Elmer Lambda 950 spectrometer. Photoluminescence measurements were done on an Edinburgh Instruments FLSP920 UV-vis-NIR spectrofluorimeter. For steady-state measurements, a 450W xenon lamp was used as the excitation source. The time resolved measurements were performed using a picosecond pulsed LED (pulse width 872 ps) as the excitation source. The signals were collected with a Hamamatsu R928P PMT detector, which has a response curve between 200 and 900 nm. All steady-state emission spectra were recorded for an excitation wavelength of 365 nm and were corrected for the detector sensitivity. The time resolved measurements were performed for an excitation wavelength of 331 nm with a bandwidth of 9.4 nm, which are the characteristics of the pulsed LED, and by collecting the signal at the maximum of emission. Photoluminescence quantum yields (PLQY) of the samples were determined for an excitation wavelength of 365 nm and by comparison with Coumarin 2, which has a known PLQY of 92% in ethanol.²⁸ Blinking experiments were performed with a microluminescence setup. For these experiments, the QDs were deposited at very low concentration on a Suprasil® 2B quartz slide by spin coating. A single QD was excited using a pulsed laser at $\lambda = 445$ nm with a repetition rate of 2.5 MHz, and the emission of the QD was detected using a PerkinElmer photon counting diode (model SPCM-AQRH). Raman spectroscopy was used to study the internal structure of the core-shell QDs. Raman spectra were recorded in backscattering geometry using a Dilor XY800 triple monochromator Raman spectrometer with an N₂ cooled charge-coupled-device detector. Laser excitation was provided by the 488 nm line of an Ar⁺-laser (Coherent). Each spectrum was calibrated with respect to neon and argon lines. This set-up provides an accuracy of the Raman shift of ± 0.4 cm⁻¹. The samples were prepared by dropcasting the QD solutions on Si wafers. After solvent evaporation, the wafers were transferred to a commercial cryostat (Oxford Instruments). All Raman measurements were performed at liquid helium temperature.

RESULTS AND DISCUSSION

Influence of oleic acid. During preliminary experiments and in a first attempt to synthesize CdSe/CdS dot-in-dots, we used the same amount of carboxylic acid (oleic acid) as of phosphonic acids (octadecylphosphonic acid and hexadecylphosphonic acid) reported in the method of Carbone *et al.* for the synthesis of CdSe/CdS dot-in-rods.²² This means no excess of OA and just the two equivalents necessary to dissolve the amount of CdO. The TEM image of the result (Figure 1a) immediately revealed that this simple modification of

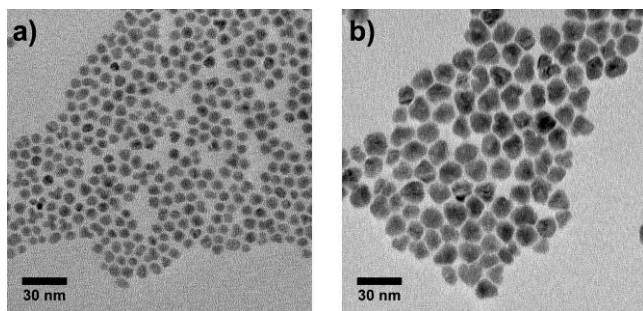


Figure 1. TEM images of CdSe/CdS QDs synthesized without OA excess (a) and with OA excess (b).

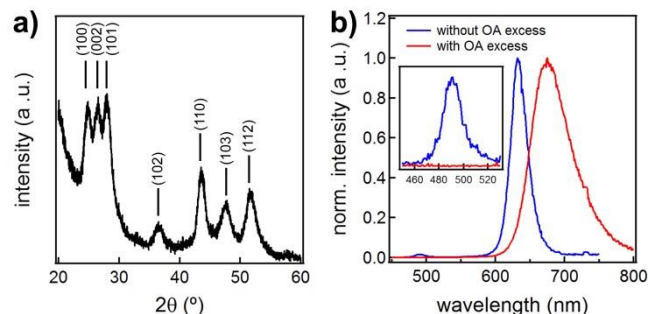


Figure 2. (a) Typical XRD diffractogram of CdSe/CdS QDs. (b) Emission spectra of CdSe/CdS QDs synthesized with and without OA excess (inset: magnification of the wavelength range 450 to 530 nm). The emission spectra were recorded for an excitation wavelength of 365 nm.

the synthesis protocol led to the formation of spherical QDs. As a matter of fact, compared to phosphonic acids, oleic acid binds more loosely²⁹ and not selectively to the different facets of wurtzite CdSe nanocrystals.³⁰ Thus, the use of oleic acid results in an isotropic growth of the CdS shell instead of the preferential growth along the wurtzite *c*-axis observed with phosphonic acids.²² XRD analyses evidenced that the CdSe/CdS dot-in-dots have a wurtzite structure (Figure 2a), indicating an epitaxial growth of the CdS shell on the wurtzite CdSe cores. The emission spectrum of this first sample (Figure 2b) featured, in addition to the main emission peak centered at 632 nm, another peak at 490 nm (inset Figure 2b). As the emission of the injected 4 nm sized CdSe cores should appear at around 600 nm, we attribute this peak to CdS nanocrystals, homogeneously nucleated during the reaction. Thus, even if the use of a carboxylic acid successfully promoted the isotropic growth of a CdS shell, the synthesis of CdSe/CdS dot-in-dots still needed optimization. To prevent the nucleation of separate CdS QDs, the synthesis was repeated using an excess of 4 mmol of OA. The TEM image (Figure 1b) shows that the resulting QDs have a larger size than when synthesized without OA excess (16 and 8 nm respectively for 4 nm cores in both cases). In this case, all the cadmium was consumed for the formation of the shell. Due to the thicker CdS shell, the emission spectrum of the CdSe/CdS QDs synthesized with an excess of OA shifted to longer wavelengths (Figure 2b). More importantly, the emission spectrum of this sample does not show any additional peak, confirming that there is no homogeneous nucleation of separate CdS QDs. Thus, an excess of OA was necessary to prevent the formation of individual CdS QDs. This result is in line with the idea that an excess of acid

increases the solubility of the growth species,³¹ which will favor shell growth over homogeneous nucleation. Additional preliminary experiments showed that the concentration of sulfur did not play any important role unless it was introduced in a more than 6-fold excess compared to cadmium. In this case, the syntheses resulted in highly polydisperse particles. Thus, only the effect of Cd concentration was investigated and is reported in the following.

Tuning the thickness of the CdS shell. To investigate the effect of cadmium concentration, CdSe/CdS QDs were synthesized starting from 2.5 nm and 3.5 nm sized wurtzite CdSe cores, and using different amounts of CdO as summarized in Table 1. Figure 3 shows the TEM images and size distributions of samples QD1, QD2 and QD3 (see Supporting Information Figure S1 for samples QD4 to QD6). In Figure 4a, the average diameters of the CdSe/CdS QDs, determined from TEM images, are plotted against the amount of cadmium used. It appears that the size of the QDs, *i.e.* the thickness of the CdS shell, increases with the amount of cadmium involved in the synthesis. As illustrated in figure 3d the dispersion of the size distribution increases with the thickness of the CdS shell. More precisely, the volume of the CdS shell reported on Figure 4b increases linearly with the amount of cadmium. The experimental sizes/volumes were always found to be in good agreement with the theoretical ones, indicating that all the cadmium introduced in the synthesis has reacted. Thus, owing to this full chemical yield of the shell formation reaction, the thickness of the CdS shell can be efficiently controlled by modifying the initial amount of CdO. In addition, the process is considerably faster than what is reported in the literature up to date. For example, a 6.7 nm thick shell (samples QD3 and QD6) corresponding to ca. 20 MLs of CdS was grown in no more than 3 minutes, whereas it could have taken up to several days to obtain the same result using the SILAR method.¹²

Table 1. Synthesis details, structural parameters and spectroscopy data of CdSe/CdS QDs synthesized with different core sizes and different amounts of CdO. The amount of TOPO was always 3 g, the OA was introduced with an excess of 4 mmol and the sulfur was in 3 to 4-fold excess compared to cadmium in all the syntheses.

sample	core size (nm)	CdO (mmol)	size (nm)	number of CdS MLs	em. peak (nm)	FWHM (nm)	τ_1 (ns)	τ_2 (ns)	PLQY (%)
QD1	2.5	0.50	8.9 ± 1.3	9.5	597	34	5	24	40
QD2	2.5	1.33	13.0 ± 1.4	15.6	623	54	30	100	26
QD3	2.5	2.67	15.8 ± 2.7	19.7	635	63	32	145	11
QD4	3.5	0.71	9.5 ± 1.2	8.9	631	36	7	33	47
QD5	3.5	1.73	13.4 ± 1.4	14.7	647	48	30	117	31
QD6	3.5	3.47	16.8 ± 3.1	19.7	653	67	42	191	15

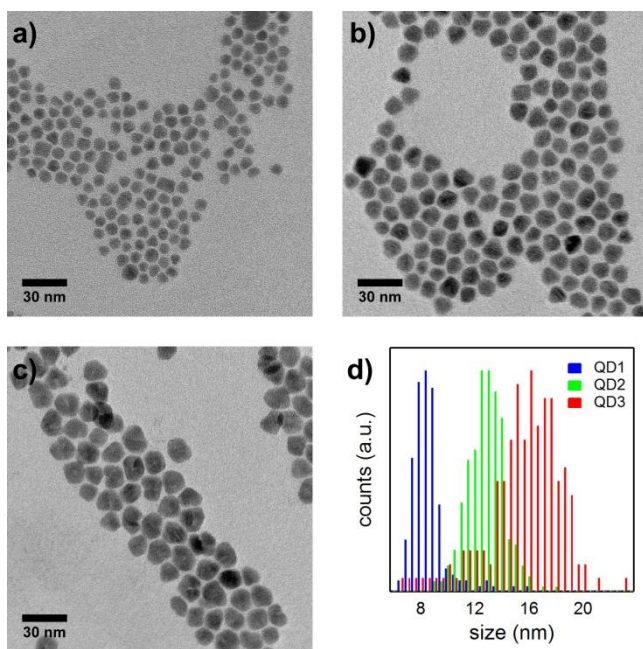


Figure 3. TEM images of samples QD1 (a), QD2 (b) and QD3 (c). Size distribution of those three samples (d) (see Supporting Information Figure S1 for samples QD4 to QD6).

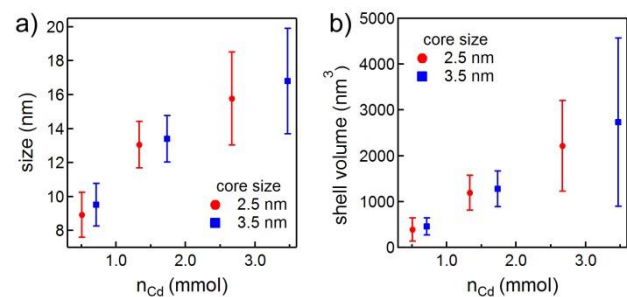


Figure 4. Average sizes (a) and volumes (b) of the CdSe/CdS QDs depending on the amount of cadmium used and for different core sizes.

Raman analysis of the CdSe/CdS QDs. Besides enhanced passivation, core-shell structures have also proven to be of interest for reducing the Auger recombination rate, which plays a role in blinking processes and multi-exciton recombi-

nation.¹³ This is thought to be linked to a graded interface resulting from an alloying of the core-shell interfacial region.³² We recently demonstrated the potential of Raman spectroscopy to investigate the structure of this interface.³³ Thus, we applied Raman spectroscopy on the ‘flash’ CdSe/CdS heteronanostructures. Samples with thicker CdS shells show mostly a bulk-like CdS vibration and the CdSe-related features are relatively weak, making a detailed discussion difficult (see Supporting Information, Figure S2). Figure 5a shows the Raman spectrum of the two exemplary samples with moderately thick shells, QD1 and QD4. The intensities were normalized to the CdS-related peak around 300 cm^{-1} . The spectra feature CdS- and CdSe-related Raman modes and (mixed) overtones. On one hand, the CdS-related peaks are not significantly different between the two samples. This also applies to the first CdS-overtone around 600 cm^{-1} . The region in between fundamental and overtone shows CdSe-CdS combined modes. The proximity of the fundamental CdS-related peak to the CdS longitudinal optical phonon (LO) bulk frequency (305 cm^{-1})³⁴ indicates a homogeneous shell with possible strain due to the lattice mismatch being mostly relaxed through the outer layers. On the other hand, the CdSe-related peaks are subject to stronger changes between the different samples. Figure 5b displays the Raman spectra limited to the frequency range of the CdSe-related vibrations. The spectra were normalized to the most prominent peak around 212 cm^{-1} . This peak is asymmetric and can be only well described by the sum of three Lorentzian functions. The background was accounted for with a linear function and a single Lorentzian function for the CdS shoulder at higher wavenumbers. The three underlying components for each sample are included in the figure. The peaks are significantly shifted in frequency, relative to bulk and between the samples. The most prominent feature around 216 cm^{-1} can be attributed to the CdSe LO.³³ Its shift relative to the bulk LO frequency (212 cm^{-1})³⁵ can be understood by a significant amount of compressive strain being present in the lattice. As the amount of core material is comparably small, the strain caused by the lattice mismatch between CdSe and CdS cannot relax and average out as it is the case for the CdS shell. Then, the strain – and related frequency shift – is different between the samples due to difference in core size and shell thickness. The shoulder below 200 cm^{-1} can be attributed to surface optical phonon (SO) which exist in finite sized crystals.^{36, 37} The third feature, the shoulder around 209 cm^{-1} was previously attributed to an intrinsic vibration of a Cd(Se,S) alloy, stemming from a significant amount of alloyed material at the interface between the CdSe core and the CdS shell.³³ The

intensity of this mode relative to the respective CdSe LO intensity is different between the samples, probably due to a comparable amount of alloyed material relative to a different amount of core material. This is in line with the different core diameters, and thus different surface/volume ratios, between the two samples. A comparison with the spectra discussed in the previous work about SILAR particles³³ suggests a similar interface composition, though the thickness of the interfacial layer cannot be estimated based on the available data. Thus, despite the fact that the reaction takes place in only 3 minutes, these Raman analyses show that the atoms at the core-shell interface still have enough time to rearrange and form alloyed layers, just as in other synthesis methods.

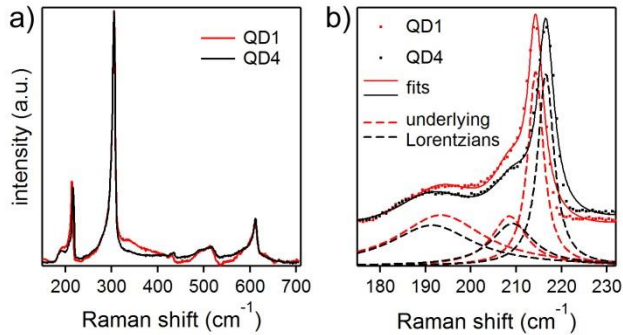


Figure 5. (a) Raman spectra of sample QD1 and QD4. (b) Focus on the CdSe-related peaks.

Optical properties of the CdSe/CdS QDs. The optical properties, *i.e.* wavelength position of the emission peak, full width at half maximum (FWHM), lifetimes (τ_1 and τ_2) and PLQY of all the samples are reported in Table 1. The exact peak wavelength of the first excitonic absorption peak could hardly be determined, especially in the case of large CdS shell thicknesses. Indeed, as illustrated in Figure 6a and its inset for samples QD1 to QD3 (see Supporting Information Figure S3 for samples QD4 to QD6), the absorption spectra of the QDs are largely dominated by the absorption of the CdS, which represents most of the volume fraction of the QDs. For illustration, the emission spectra of samples QD1 to QD3 are shown in Figure 6b (see Supporting Information Figure S3 for samples QD4 to QD6). As expected, the emission spectra of the CdSe/CdS QDs shift towards longer wavelengths when the thickness of the CdS shell increases. This is due to the delocalization of the electron from the core into the shell following the small conduction band offset between CdSe and CdS. Figure 6b also shows that the emission peak becomes broader when the thickness of the CdS increases. Indeed, the FWHM values, which are reported in Table 1, reflect the concomitant increase of the size distribution already observed in Figure 3d. Nevertheless, even for the largest QDs the FWHM was always below 70 nm, which is suitable for many optical applications. From point of view of the photoluminescence lifetime, the decays reported in Figure 6c for samples QD1 to QD3 (see Supporting Information, Figure S3 for samples QD4 to QD6) were fitted with a double exponential. A short lifetime (τ_1) and a longer one (τ_2) were obtained for each samples and these values are reported in Table 1. The short lifetime can fairly be attributed to non-radiative processes involving the surface of the nanocrystals, and the longer lifetime corresponds most likely to the excitonic recombination. As expected, the growth of thicker CdS shells results in an increase of both lifetimes,

which is due to a decrease of the overlap of the exciton wave functions. As for the red shift of the emission spectra, due to a smaller offset between the conduction bands of the CdSe and the CdS shell, the electrons are delocalized in the entire volume of the QD whereas the holes remain mainly confined in the core.¹¹ We did not observe any plateau value of the lifetime as reported by Ghosh *et al.*, even if some of our shell volumes were larger than the 750 nm³ threshold value these authors reported.¹² In core-shell QDs, with the highest PLQY values typically being observed for 2-3 monolayers, the subsequent PLQY decrease with additional shell layers is often explained by higher strain and defect densities induced by lattice mismatch or incoherent growth of thicker shells.¹⁸⁻²⁰ The CdSe/CdS QDs reported here showed PLQYs of 40-50% in the case of shells corresponding to about 9 CdS MLs (samples QD1 and QD4), 25-30% in the case of shells corresponding to about 15 CdS MLs (samples QD2 and QD5) and still 10-15% for QDs with up to almost 20 CdS MLs (samples QD3 and QD6). At similar shell thicknesses, these PLQY values are comparable or even higher than those obtained with a fully optimized SILAR procedure.¹² This is probably a benefit of the high synthesis temperature that allows a continuous coherent growth of the CdS shell, resulting in nanocrystals with high crystallinity.

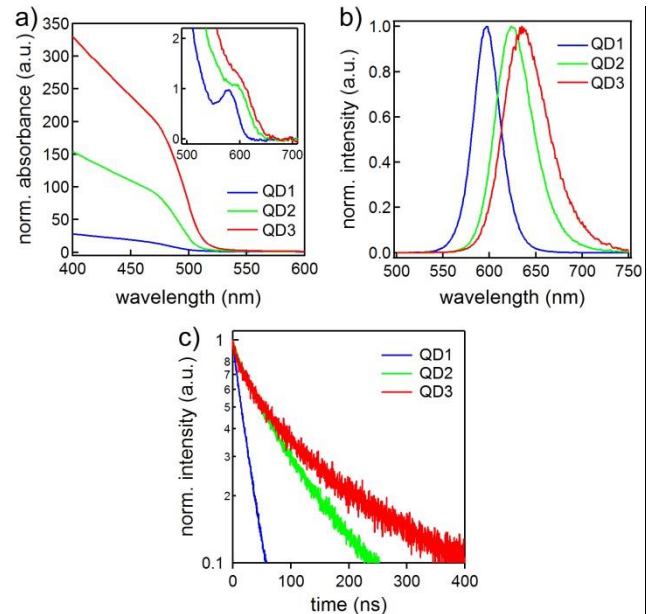


Figure 6. Normalized (a) absorption spectra, (b) emission spectra, and (c) photoluminescence decays of samples QD1, QD2 and QD3 (see Supporting Information Figure S3 for samples QD4 to QD6). The emission spectra were recorded for an excitation wavelength of 365 nm. The photoluminescence decays were recorded for an excitation wavelength of 331 nm.

In addition to the sharp and bright emission, CdSe/CdS QDs prepared with this ‘flash’ synthesis can show very low blinking behavior. In Figure 7 single QD measurements are reported for sample QD5. To ensure that the measured emission originated from a single photon emitter, anti-bunching experiments were performed (see Supporting Information, Figure S4). In Figure 7, the black curves represent the intensity of the luminescence, *i.e.*, the number of detected photons per time-bin of 10 ns, as a function of time, and the red curves show the corresponding statistical distribution of the number of

counts. In Figure 7a, the fluence of each excitation pulse was set to produce an average number of $v_{av} = 0.15$ excitons per pulse. During the 400 s of the record not a single off-period has been seen. In addition, the statistical distribution of the number of counts is single-peaked and has a mean value of 107 ± 21.2 counts. The fact that the distribution is broader than a Poisson distribution indicates that, despite no off-period is seen, the PLQY randomly changes in time by about 10% of its average value. These fluctuation periods are clearly seen on the black curves (Figure 7). Schlegel *et al.* already reported that fluctuating dynamic quenching processes could occur even at a single QD level depending on its local gaseous environment.³⁸ Indeed, photoluminescence measurements of QDs in different controlled atmospheres already showed that both water or oxygen molecules can have independent and synergistic effects on their optical properties.³⁹ Figure 7b shows the luminescence of the same QD, but using a stronger excitation ($v_{av} = 0.56$). The QD again emits without intermittency during 400 s except for a short time interval of a few seconds around $t = 242$ s. In Figure 7b, the displayed time interval is reduced for a better visualization of the off-period. The statistics of the number of counts per 10-ms time-bin now shows a double-peaked structure. The main peak (394 ± 86 counts) corresponds to the on-state while the small one (47 ± 10 counts) corresponds to the off-state. Thus, it appears that, despite the high excitation level, nearly no blinking occurred. A further increase of the excitation power tended to increase the duration of the off-periods which were nevertheless limited. It appears that the Auger processes responsible for blinking are strongly, if not completely, suppressed in the CdSe/CdS ‘flash’ QDs. This can be explained by the very thick CdS shell and the delocalization of the electron in this very large volume.¹⁰⁻¹² Chen *et al.* already reported a low blinking behavior of CdSe/CdS QDs with similar shell thickness.¹⁰ However, we could achieve a similar result with a 3 minutes synthesis instead of several days using the SILAR approach. Furthermore, the observed alloyed interface between the CdSe core and CdS is of importance. García-Santamaría *et al.* recently demonstrated the importance of these alloyed interfaces on the reduction of Auger recombination through a “smoothing” of the confinement potential.¹³ A smoothing of this potential was also reported by Wang *et al.* as an important parameter for the absence of blinking in their CdZnSe alloyed QDs coated with ZnSe shells.⁹ More recently, Bawendi *et al.* reported non-blinking CdSe/CdS QDs with relatively thin CdS shells,⁴⁰ claiming that this was the result of the high synthesis temperature (310 °C) and the slow CdS formation which produces highly crystalline shells. The ‘flash’ CdSe/CdS QDs combine most of these characteristics, *i.e.* thick CdS shells, alloyed interfaces and high crystallinity thanks to high synthesis temperature, which explains the low blinking observed.

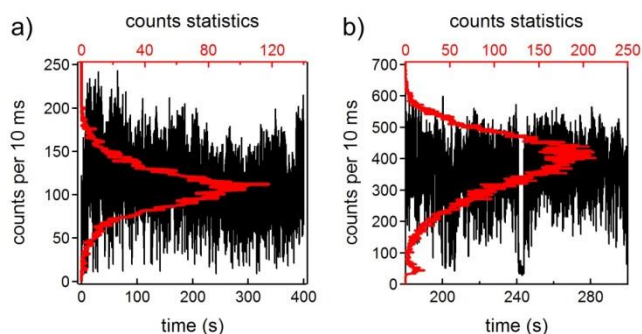


Figure 7. : Luminescence intensity (black line, left axis) of a single CdSe/CdS QD as a function of time (bottom axis) for (a) $v_{av} = 0.15$ and (b) $v_{av} = 0.56$. The intensity of the luminescence is measured by the number of counts recorded by a photon counter during 10-ms time intervals. The statistical distribution of the number of counts is shown in red (top axis). In (b) the time interval is reduced for better visualization of the off-state, but the counts statistics (red line) are still calculated based on a 400 s experiment.

CONCLUSION

In conclusion, a new fast and efficient method for the synthesis of CdSe/CdS core-shell QDs was successfully developed. In this method, referred to as ‘flash’ synthesis, the use of a carboxylic acid (OA) instead of phosphonic acids led to the isotropic growth of CdS shells on wurtzite CdSe cores. It was found that an excess of OA compared to cadmium was necessary to prevent the secondary nucleation of individual CdS QDs. The thickness of the CdS shell could then be easily tuned by changing the amount of cadmium involved in the synthesis. This reaction is very fast, with full chemical yield, allowing the growth of very thick shell (up to 6.7 nm in the present study) in no more than 3 minutes. The synthesized CdSe/CdS QDs showed narrow emissions with enhanced PLQY even for very thick CdS shells. Finally, Raman spectroscopy analyses evidenced an alloying of the interface between the CdSe core and the CdS shell, which together with the thick CdS shell and probable high crystallinity, resulted in an important reduction of the Auger recombination and therefore of the blinking behavior as evidenced by single QD measurements for long periods. These QDs are therefore very promising for many applications where optical properties need to remain stable, such as lasing or biolabeling.

ASSOCIATED CONTENT

Supporting Information. Additional TEM images, Raman spectra, UV-vis absorption spectra, photoluminescence spectra, photoluminescence decays and anti-bunching experiment. This material is available free of charge via the Internet at <http://pubs.acs.org>.

AUTHOR INFORMATION

Corresponding Author

*E-mail: zeger.hens@ugent.be.

NOTES

The authors declare no competing financial interest.

ACKNOWLEDGMENT

The authors acknowledge BelSPo (IAP 7.35, photonics@be), FWO-Vlaanderen (Project G.0760.12), German Research Foundation (Project LA 2901/1-1), Max Kade Foundation, and Hercules Foundation (project AUGE/09/024 “Advanced Luminescence Setup”) for financial support.

REFERENCES

- (1) McDonald, S. A.; Konstantatos, G.; Zhang, S.; Cyr, P. W.; Klem, E. J. D.; Levina, L.; Sargent, E. H. *Nat. Mater.* **2005**, *4*, 138-142.

- (2) Caruge, J. M.; Halpert, J. E.; Wood, V.; Bulovic, V.; Bawendi, M. G. *Nat. Photonics* **2008**, *2*, 247-250.
- (3) Michalet, X.; Pinaud, F. F.; Bentolila, L. A.; Tsay, J. M.; Doose, S.; Li, J. J.; Sundaresan, G.; Wu, A. M.; Gambhir, S. S.; Weiss, S. *Science* **2005**, *307*, 538-544.
- (4) Medintz, I. L.; Uyeda, H. T.; Goldman, E. R.; Mattoussi, H. *Nat. Mater.* **2005**, *4*, 435-446.
- (5) Lee, S. F.; Osborne, M. A. *ChemPhysChem* **2009**, *10*, 2174-2191.
- (6) Frantsuzov, P.; Kuno, M.; Janko, B.; Marcus, R. A. *Nat. Phys.* **2008**, *4*, 519-522.
- (7) Heyes, C. D.; Kobitski, A. Y.; Breus, V. V.; Nienhaus, G. U. *Phys. Rev. B* **2007**, *75*, 125431.
- (8) Hollingsworth, J. A. *Chem. Mater.* **2013**, *25*, 1318-1331.
- (9) Wang, X.; Ren, X.; Kahen, K.; Hahn, M. A.; Rajeswaran, M.; Maccagnano-Zacher, S.; Silcox, J.; Cragg, G. E.; Efros, A. L.; Krauss, T. D. *Nature* **2009**, *459*, 686-689.
- (10) Chen, Y.; Vela, J.; Htoon, H.; Casson, J. L.; Werder, D. J.; Bussian, D. A.; Klimov, V. I.; Hollingsworth, J. A. *J. Am. Chem. Soc.* **2008**, *130*, 5026-5027.
- (11) Mahler, B.; Spinicelli, P.; Buil, S.; Quelin, X.; Hermier, J.-P.; Dubertret, B. *Nat. Mater.* **2008**, *7*, 659-664.
- (12) Ghosh, Y.; Mangum, B. D.; Casson, J. L.; Williams, D. J.; Htoon, H.; Hollingsworth, J. A. *J. Am. Chem. Soc.* **2012**, *134*, 9634-9643.
- (13) García-Santamaría, F.; Brovelli, S.; Viswanatha, R.; Hollingsworth, J. A.; Htoon, H.; Crooker, S. A.; Klimov, V. I. *Nano Lett.* **2011**, *11*, 687-693.
- (14) Li, J. J.; Wang, Y. A.; Guo, W.; Keay, J. C.; Mishima, T. D.; Johnson, M. B.; Peng, X. *J. Am. Chem. Soc.* **2003**, *125*, 12567-12575.
- (15) Mekis, I.; Talapin, D. V.; Kornowski, A.; Haase, M.; Weller, H. *J. Phys. Chem. B* **2003**, *107*, 7454-7462.
- (16) Guo, Y.; Marchuk, K.; Sampat, S.; Abraham, R.; Fang, N.; Malko, A. V.; Vela, J. *J. Phys. Chem. C* **2011**, *116*, 2791-2800.
- (17) van Embden, J.; Jasieniak, J.; Mulvaney, P. *J. Am. Chem. Soc.* **2009**, *131*, 14299-14309.
- (18) Dabbousi, B. O.; Rodriguez-Viejo, J.; Mikulec, F. V.; Heine, J. R.; Mattoussi, H.; Ober, R.; Jensen, K. F.; Bawendi, M. G. *J. Phys. Chem. B* **1997**, *101*, 9463-9475.
- (19) Talapin, D. V.; Mekis, I.; Götzinger, S.; Kornowski, A.; Benson, O.; Weller, H. *J. Phys. Chem. B* **2004**, *108*, 18826-18831.
- (20) Lu, Y.; Zhang, Y. Q.; Cao, X. A. *Appl. Phys. Lett.* **2013**, *102*, 023106-023104.
- (21) Veilleux, V.; Lachance-Quirion, D.; Doré, K.; Landry, D. B.; Charette, P. G.; Ni Allen, C. *Nanotechnology* **2010**, *21*, 134024.
- (22) Carbone, L.; Nobile, C.; De Giorgi, M.; Sala, F. D.; Morello, G.; Pompa, P.; Hytch, M.; Snoeck, E.; Fiore, A.; Franchini, I. R.; Nadasan, M.; Silvestre, A. F.; Chiodo, L.; Kudera, S.; Cingolani, R.; Krahne, R.; Manna, L. *Nano Lett.* **2007**, *7*, 2942-2950.
- (23) Talapin, D. V.; Nelson, J. H.; Shevchenko, E. V.; Aloni, S.; Sadtler, B.; Alivisatos, A. P. *Nano Lett.* **2007**, *7*, 2951-2959.
- (24) Fiore, A.; Mastria, R.; Lupo, M. G.; Lanzani, G.; Giannini, C.; Carlino, E.; Morello, G.; De Giorgi, M.; Li, Y.; Cingolani, R.; Manna, L. *J. Am. Chem. Soc.* **2009**, *131*, 2274-2282.
- (25) Hewa-Kasakarage, N. N.; Kirsanova, M.; Nemchinov, A.; Schmall, N.; El-Khoury, P. Z.; Tarnovsky, A. N.; Zamkov, M. *J. Am. Chem. Soc.* **2009**, *131*, 1328-1334.
- (26) Jasieniak, J.; Smith, L.; Embden, J. v.; Mulvaney, P.; Califano, M. *J. Phys. Chem. C* **2009**, *113*, 19468-19474.
- (27) Čapek, R. K.; Moreels, I.; Lambert, K.; De Muynck, D.; Zhao, Q.; Van Tomme, A.; Vanhaecke, F.; Hens, Z. *J. Phys. Chem. C* **2010**, *114*, 6371-6376.
- (28) Montalti, M.; Credi, A.; Luca, P.; Gandolfi, T. M., *Handbook of Photochemistry, 3rd edition*. CRC Press: 2006.
- (29) Gomes, R.; Hassinen, A.; Szczygiel, A.; Zhao, Q.; Vantomme, A.; Martins, J. C.; Hens, Z. *J. Phys. Chem. Lett.* **2011**, *2*, 145-152.
- (30) Rempel, J. Y.; Trout, B. L.; Bawendi, M. G.; Jensen, K. F. *J. Phys. Chem. B* **2006**, *110*, 18007-18016.
- (31) Abe, S.; Capek, R. K.; De Geyter, B.; Hens, Z. *ACS Nano* **2013**, *7*, 943-949.
- (32) Cragg, G. E.; Efros, A. L. *Nano Lett.* **2009**, *10*, 313-317.
- (33) Tschirner, N.; Lange, H.; Schliwa, A.; Biermann, A.; Thomsen, C.; Lambert, K.; Gomes, R.; Hens, Z. *Chem. Mater.* **2012**, *24*, 311-318.

- (34) Cadmium sulfide (CdS) phonon wavenumbers, mean square displacements. In *Landolt-Börnstein - Group III Condensed Matter; Numerical Data and Functional Relationships in Science and Technology*, Madelung, O.; Rössler, U.; Schulz, M., Eds. Vol. 41B.
- (35) Cadmium selenide (CdSe) phonon wavenumbers, mean square displacements. In *Landolt-Börnstein - Group III Condensed Matter; Numerical Data and Functional Relationships in Science and Technology*, Madelung, O.; Rössler, U.; Schulz, M., Eds. Vol. 41B.
- (36) Comas, F.; Studart, N.; Marques, G. E. *Solid State Commun.* **2004**, *130*, 477-480.
- (37) Lange, H.; Artemyev, M.; Woggon, U.; Thomsen, C. *Nanotechnology* **2009**, *20*, 045705.
- (38) Schlegel, G.; Bohnenberger, J.; Potapova, I.; Mews, A. *Phys. Rev. Lett.* **2002**, *88*, 137401.
- (39) Pechstedt, K.; Whittle, T.; Baumberg, J.; Melvin, T. *J. Phys. Chem. C* **2010**, *114*, 12069-12077.
- (40) Chen, O.; Zhao, J.; Chauhan, V. P.; Cui, J.; Wong, C.; Harris, D. K.; Wei, H.; Han, H.-S.; Fukumura, D.; Jain, R. K.; Bawendi, M. G. *Nat. Mater.* **2013**, *12*, 445-451.

Insert Table of Contents artwork here

